

## Complex Phase Behavior of Repulsive Step Potential Systems in Three Dimensions

Yu. D. Fomin, N. V. Gribova, and V. N. Ryzhov

Institute for High Pressure Physics, Russian Academy of Sciences, Troitsk 142190, Moscow Region, Russia

Daan Frenkel

FOM Institute for Atomic and Molecular Physics, Amsterdam, The Netherlands

S. M. Stishov

Institute for High Pressure Physics, Russian Academy of Sciences, Troitsk 142190, Moscow Region, Russia and Los Alamos National Laboratory, 87545 Los Alamos, NM, USA  
(Dated: March 23, 2024)

The comprehensive computer simulation study of the phase diagram of the repulsive step potential system in three dimensions is represented. We show that the system with a simple purely repulsive isotropic potential demonstrates a number of unusual features. The maximum and minimum on the melting curve are found for some regions of potential parameters. It is shown that the phase diagram in  $P$ - $T$  plane includes two isostructural crystalline parts separated by the disordered phase which is amorphous at low enough temperatures. Phase diagram in the  $(P-T)$  plane shows that the transition to the amorphous state occurs approximately along the extrapolated spinodals. Structural FCC-BCC phase transition is found at high densities.

PACS numbers: 61.20.Gy, 61.20.Ne, 64.60.Kw

After the pioneering work by Hemmer and Stell [1], where the soft core potential with an attractive interaction at large distances was first proposed for the qualitative explanation of the isostructural phase transitions in materials such as Ce or Cs, a lot of attention was paid to the investigation of the properties of the systems with the potentials that have a region of negative curvature in their repulsive core [2, 3, 4, 5, 6, 7, 8, 9, 10, 11, 12, 13, 14, 15, 16, 17, 18, 19]. These studies are particularly relevant because the interatomic potentials of some pure metallic systems, metallic mixtures, electrolyte and colloidal systems can be approximated by such type of potentials. The simplest form of the negative curvature potential is the repulsive step potential which consists of a hard core plus a finite repulsive shoulder of a larger radius. It is well known that systems of particles interacting through the pair potentials which have repulsive shoulders can possess a rich variety of phase transitions and thermodynamic anomalies, including water-like anomalies [8], liquid-liquid phase transitions [5, 6, 7] and isostructural transitions in the solid region [16, 17, 18]. The features of greatest interest in the experimental phase diagrams of Ce and Cs are the isostructural solid-solid phase transitions and the melting temperature minimum and maximum. The authors of Ref. [16, 17] succeeded in modeling these features of the phase diagram in two dimensions.

In this paper we present results, based on computer simulations in three dimensions, of the phase behavior of the system with the purely repulsive step potential which reveal a surprisingly complex phase behavior of the system as a function of the potential parameters and show new features not found in previous studies.

The repulsive step potential has the form :

$$(r) = \begin{cases} < 1; & r < d \\ & & d < r \\ 0; & r > \end{cases} \quad (1)$$

and is characterized by the hard core diameter  $d$ , the width of the repulsive step  $\sigma$  and its height  $\epsilon$ . In the low temperature  $T \ll \epsilon$  and high temperature  $T \gg \epsilon$  limits the system behaves like a simple hard sphere system with hard-sphere diameter  $d$  or  $d + \sigma$  correspondingly. Schematic phase diagram may be understood in the following way: the melting line of the hard sphere system has the form  $P = cT^\alpha$ , where  $c \approx 12$  and  $\alpha$  is a hard sphere diameter. At low and high temperature limits one has two straight melting lines which correspond to hard spheres with diameters  $d$  and  $d + \sigma$ . At higher temperatures and densities the line corresponding to  $d + \sigma$  should bend to the line corresponding to the hard spheres with the diameter  $d$ . These lines merge at  $T = \epsilon$  and, depending on the magnitude of the ratio  $s = \sigma/d$  one can expect more or less pronounced anomalies in this region. For high values of  $s$  one can expect well pronounced maximum on the resulting melting curve which should disappear in the limit  $s \rightarrow 1$  [19].

In our simulations we have used a smoothed version of the repulsive step potential (1), which has the form :

$$(r) = \frac{d^n}{r^n} + \frac{1}{2} \epsilon (1 - \tanh(k_0(r - s))) \quad (2)$$

where  $n = 14$ ;  $k_0 = 10$ . We have considered the following values of  $s$ :  $s = 1.55; 1.35; 1.15$ . Further in this paper we use the dimensionless quantities:  $r = r/d$ ,  $P^* = P d^3/\epsilon$ ;  $V^* = V/N d^3 = 1/\rho^*$ ;  $T^* = k_B T/\epsilon$ , omitting the tilde marks.

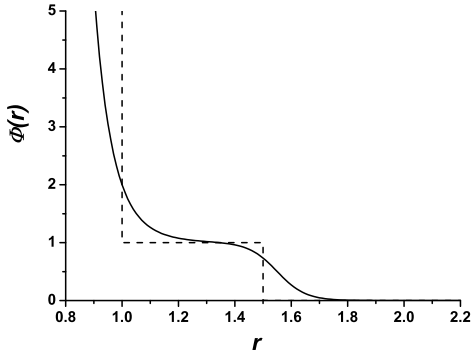


FIG. 1: A repulsive step potential consisting of a hard core plus a finite shoulder (dashed line) ( $\sigma = 1$ ;  $\sigma_s = 1.5$ ) along with the continuous version of the potential (2) used in the simulations ( $\sigma = 1$ ;  $\sigma_s = 1.55$ ).

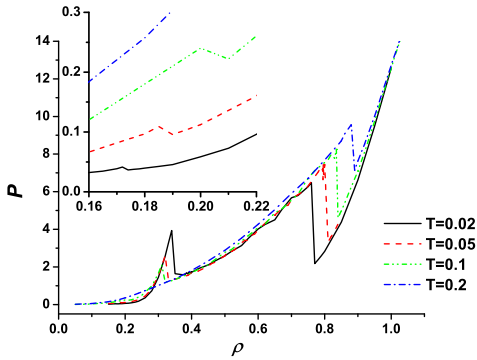


FIG. 2: The family of pressure isotherms for the purely repulsive step potential (2) for  $\sigma_s = 1.55$ .

In Fig. 1 the repulsive step potential is shown along with its smooth version which was used in our Monte-Carlo and molecular dynamics simulations.

In order to investigate phase diagrams of the system with the potential (2) we studied isotherms, isochores, radial distribution functions (RDF), mean-square displacements (MSD), positional order parameter (POP) in the framework of the standard molecular dynamics in the NVT ensemble with periodic boundary conditions. Temperature is fixed by rescaling the velocities of the particles whenever necessary [21]. Pressure is calculated by a direct evaluation in terms of interparticle forces. To obtain RDF, MSD and POP, we started from the lattice structure (FCC or BCC), equilibrated for  $5 \cdot 10^6$  cycles and then measured for  $3 \cdot 10^6$  cycles with a time step  $\tau = 5 \cdot 10^{-5}$ , or from disordered phase obtained by starting from the crystal one at high temperature and low density. In some cases the system demonstrates glassy behavior therefore equilibration run had to be so long.

We also calculated Helmholtz free energy of the sys-

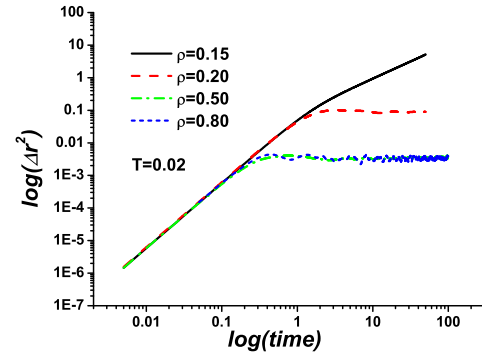
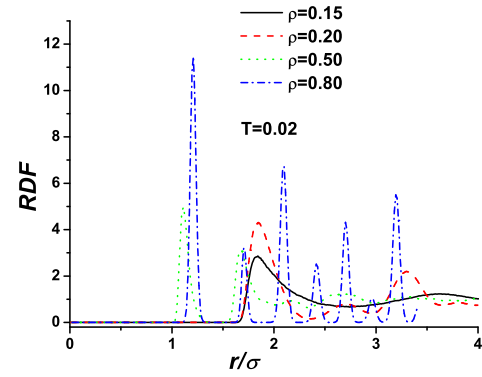


FIG. 3: RDF (upper figure) and MSD for different densities at  $T = 0.02$ .

tem using the thermodynamic integration in the framework of NVT ensemble Monte Carlo simulations [21]. For calculating the free energy of a liquid phase we used integration from dilute gas limit [21]. Solid phase free energy was calculated by coupling with Einstein crystal (Frenkel-Add method) [21, 22]. We did  $10^6$  equilibration cycles and then 50000 production cycles.

In order to locate roughly phase boundaries for crystal phases we analyzed the behavior of RDF, MSD and POP in the vicinity of van der Waals loops on the isotherms using MD simulations. In Fig. 2 the family of pressure isotherms for the purely repulsive step potential (2) with  $\sigma_s = 1.55$  for different values of  $T$  is shown. One can see that for  $T = 0.02; 0.05; 0.1$  there are 3 sharp bends on the pressure isotherms and only one sharp bend for  $T = 0.2$ . The nature of the transitions may be understood from the behavior of RDF and MSD shown in Fig. 3 for  $T = 0.02$ . It can be seen that for  $\rho = 0.15$  (before the first bend on the corresponding isotherm) RDF and MSD have a liquid-like character. For  $\rho = 0.2$  RDF and MSD have solid-like forms. The most interesting behavior corresponds to the densities in the range between second and third bends on the isotherms. In this case (see lines corresponding to  $\rho = 0.5$ ) RDF is liquid-like, but MSD has solid-like form. This means that in the range of densi-

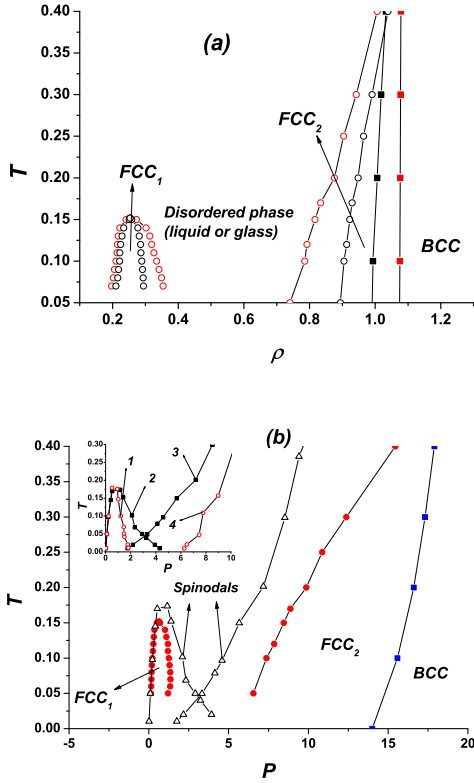


FIG. 4: Phase diagram of the system of particles interacting through the potential (2) with  $\epsilon_s = 1.55$  in  $T$  and  $P$   $T$  planes.

ties between second and third bends on the isotherms at low enough temperatures there exists an amorphous solid phase, which transforms to the crystalline solid after the third transition (see RDF and MSD for  $\epsilon = 0.8$ ). In this density region the crystalline solid is unstable against the amorphization at all temperatures. The lowest temperature at which the simulations were done was  $T = 0.00001$ . However, it may be shown that at high temperatures the system is a liquid (RDF and MSD are liquid-like). The location of the liquid-glass transition is a subject of the separate publication. This approach gives the possibility to obtain the approximate limits of stability (spinodals) of solid and liquid phases.

In Fig. 4(a) we show the phase diagram of the system with  $\epsilon_s = 1.55$  as obtained using the double tangent construction. Open circles determine the boundaries of liquid and solid ( $FCC$ ) phases. Squares correspond to the structural  $FCC$ - $BCC$  transition. As it was discussed above there are two  $FCC$  phases separated by the rather wide density range of the disordered phase which is amorphous at low temperatures. To our knowledge this is a new type of phase behavior which was not found in previous studies.

In Fig. 4(b) the phase diagram of the system with

$\epsilon_s = 1.55$  is represented in  $(T - P)$  plane. The circles correspond to the melting line obtained from the double tangent construction, and open triangles denote the spinodals obtained from MD simulations. As one can expect the spinodals lie higher in temperature than the thermodynamic transition. At higher densities there is a phase transition between  $FCC$  and  $BCC$  phases (squares). The line of the  $FCC$ - $BCC$  transition was obtained using the double tangent construction. MD simulations (RDF and POP behavior) confirm these results. The thermodynamic melting line (circles) consists of two parts which should merge at low temperatures. Unfortunately, we could not calculate the phase diagram between these parts because of problems with calculation of the Helmholtz free energy of the disordered state.

In the insert in Fig. 4(b) the stability line of the crystalline solid phase is shown by the squares. The open circles correspond to the stability limits of the disordered phases obtained from the pressure isotherms (see Fig. 2). One can see that the transitions to the amorphous phases occurs along the extrapolations of the melting lines to the supercooled region, and the "melting" in this region is nothing but the pressure induced amorphization [14, 15, 23, 24, 25]. It should be noted that due to the fact that only spinodals are shown in the insert in Fig. 4(b), we can not determine whether pressure induced amorphization is conventional "two-phase melting" or mechanical instability [14, 15, 23]. In order to explain the phase diagram shown in the insert in Fig. 4(b) let us consider the behavior of the system under compression at temperatures lower than the melting line minimum. Taking into account Fig. 2, it can be seen that upon increasing pressure one intersects the left hand part of curve 1 corresponding to the stability line of the liquid phase. At this line liquid-low-density  $FCC$  solid transition occurs. At the continuation of line 2 the transition from a low-density  $FCC$  solid to amorphous phase takes place. Line 4 corresponds to the limit of stability of the amorphous phase. At this line amorphous phase crystallizes and becomes a high-density  $FCC$  phase. Upon decompression from the high-density  $FCC$  phase one first meets the continuation of line 3 where the amorphization occurs. Right hand part of line 1 corresponds to the limit of stability of the amorphous phase, where amorphous phase crystallizes to the low-density  $FCC$  phase. Upon further decompression the  $FCC$  phase melts at the left hand part of line 2.

It should be emphasized that we can not reach true thermodynamic equilibrium state in the density range where we find the amorphous phase. In principle, the energy of the amorphous phase may be higher than the energies of  $FCC_1$  and  $FCC_2$  solids, and in this case the amorphous phase may exist only because of the very slow nonergodic kinetics of the system. If the system could be equilibrated one would find the isostructural  $FCC_1$ - $FCC_2$

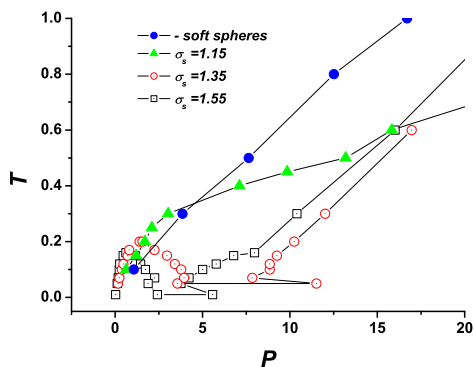


FIG. 5: Phase diagram of the systems of particles interacting through the potential (2) with  $\sigma_s = 1:15; 1:35; 1:55$  in  $T-P$  plane. Filled circles correspond to the melting line of the soft sphere potential ( $\epsilon(r) = 1-r^{14}$ ) without repulsive shoulder.

phase transition (see, for example, [18]).

In Fig. 5 the evolution of the melting line obtained by equating the Helmholtz free energies is shown as a function of the size of the repulsive step  $\sigma_s$ . It can be seen that the system behaves in qualitative accordance with the described above model of the mixture of the hard spheres with two diameters [19]. In particular, the melting curve maximum disappears for  $\sigma_s = 1:15$ . We are going to discuss this phase diagram in more details in a separate publication. For the comparison we also show the melting line of the soft sphere potential ( $\epsilon(r) = 1-r^{14}$ ) without repulsive shoulder (filled circles).

In conclusion, we performed the comprehensive computer simulation study of the phase diagram of the system described by the simple purely repulsive step potential (2) in three dimensions and found a surprisingly complex phase behavior. The maxima and minima on the melting curve are found for some regions of potential parameters. It is shown that the evolution of the phase diagram with change of the parameters may be qualitatively explained in the framework of the simple model in which the system is considered as a mixture of two types of hard spheres. For the first time it is shown that the phase diagram in  $T-P$  plane includes two FCC phases with different densities separated by the disordered phase which is amorphous at low enough temperatures. We show that the transition to the amorphous state occurs approximately along the extrapolated spinodals in the ( $P-T$ ) plane. Structural FCC-BCC phase transition is found at high densities.

We thank V. V. Brazhkin for stimulating discussions.

The work was supported in part by the Russian Foundation for Basic Research (Grants No 05-02-17280 and No 05-02-17621) and NW O-RFBR Grant No 047.016.001.

- [1] P. C. Hemmer and G. Stell, Phys. Rev. Lett. 24, 1284 (1970); G. Stell and P. C. Hemmer, J. Chem. Phys. 56, 4274 (1972).
- [2] V. V. Brazhkin, S. V. Buldyrev, V. N. Ryzhov, and H. E. Stanley [eds], New Kinds of Phase Transitions: Transformations in Disordered Substances [Proc. NATO Advanced Research Workshop, Volga River] (Kluwer, Dordrecht, 2002).
- [3] E. Velasco, L. Mederos, G. Navascues, P. C. Hemmer, and G. Stell, Phys. Rev. Lett. 85, 122 (2000).
- [4] P. C. Hemmer, E. Velasco, L. Mederos, G. Navascues, and G. Stell, J. Chem. Phys. 114, 2268 (2001).
- [5] V. N. Ryzhov and S. M. Stishov, Zh. Eksp. Teor. Fiz. 122, 820 (2002) [JETP 95, 710 (2002)].
- [6] V. N. Ryzhov and S. M. Stishov, Phys. Rev. E 67, 010201(R) (2003).
- [7] Yu. D. Fomin, V. N. Ryzhov, and E. E. Tareyeva, Phys. Rev. E 74, 041201 (2006).
- [8] M. R. Sadr-Lahijany, A. Scala, S. V. Buldyrev and H. E. Stanley, Phys. Rev. Lett. 81, 4895 (1998).
- [9] M. R. Sadr-Lahijany, A. Scala, S. V. Buldyrev and H. E. Stanley, Phys. Rev. E 60, 6714 (1999).
- [10] P. Kumar, S. V. Buldyrev, F. Sciortino, E. Zaccarelli, and H. E. Stanley, Phys. Rev. E 72, 021501 (2005).
- [11] L. Xu, S. V. Buldyrev, C. A. Angell, and H. E. Stanley, Phys. Rev. E 74, 031108 (2006).
- [12] E. A. Jagla, J. Chem. Phys. 111, 8980 (1999).
- [13] E. A. Jagla, Phys. Rev. E 63, 061501 (2001).
- [14] S. Bustingorry and E. A. Jagla, Phys. Rev. B 69, 064110 (2004).
- [15] S. Bustingorry and E. A. Jagla, Phys. Rev. B 71, 224119 (2005).
- [16] D. A. Young and B. J. Alder, Phys. Rev. Lett. 38, 1213 (1977).
- [17] D. A. Young and B. J. Alder, J. Chem. Phys. 70, 473 (1979).
- [18] P. Bolhuis and D. Frenkel, J. Phys.: Condens. Matter 9, 381 (1997).
- [19] S. M. Stishov, Phil. Mag. B 82, 1287 (2002).
- [20] W. G. Hoover, S. G. Gray, and K. W. Johnson, J. Chem. Phys. 55, 1128 (1971).
- [21] Daan Frenkel and Berend Smit, Understanding molecular simulation (From Algorithms to Applications), 2nd Edition (Academic Press), 2002.
- [22] D. Frenkel and A. J. C. Ladd, J. Chem. Phys. 81, 107 (1984).
- [23] O. Mishima, Nature (London) 384, 546 (1996).
- [24] A. G. Lyapin and V. V. Brazhkin, Phys. Rev. B 54, 12036 (1996).
- [25] E. L. Gromnitskaya, O. V. Stalgorova, V. V. Brazhkin, and A. G. Lyapin, Phys. Rev. B 64, 094205 (2001).